EMI mitigation with lossy material at 10 GHz

Xiangyang Jiao[#1], Pratik Maheshwari[#2], Victor Khikevich[#3], Paul Dixon[4], Yoeri Arien[5], Alpesh Bhobe[6],
[#]Missouri University of Science and Technology
Rolla, USA.
[1]xjn74, [2]prm8c7, [3]khikevichv, [7]jlkc9, [8]xl3df, [9]davidjp, [10]drewniak@mst.edu

Jing Li[#7], Xiao Li[#8], David Pommerenke[#9], James Drewniak[#10], Hamed Kajbaf[11], Jin Min[12]
[4]Laird Technologies, Randolph, MA, USA
[5]Laird Technologies, Geel, Belgium
[6]Cisco Systems Inc., San Jose, CA, USA
[11,12]Amber Precision Instruments, Sunnyvale, CA, USA
[4]paul.dixon, [5]yoeri.arien@lairdtech.com,
[6]abhobe@cisco.com, [11]hamed, [12]jinmin@amberpi.com

***Abstract*—In this paper, absorber material is utilized to mitigate an EMI problem in real hardware. For a complex and large system, identification of the source location is the first problem which must be solved to achieve electromagnetic interference (EMI) mitigation. Emission Source Microscopy (ESM) provides a powerful tool for locating the sources of radiation in GHz range on a printed circuit board (PCB). Once the source is identified, a suitable volume of the absorber material is placed on the source location to effectively reduce the radiated power at the frequency of interest. Further measurements of the total radiated power in a reverberation chamber are also performed to validate the EMI reduction method with the absorber material.**

***Keywords*— Absorber material**; **Emission source microscopy**; **Source localization**; **EMI.**

I. INTRODUCTION

Due to the increase in the operating speed and decrease in the size of a typical IC chip, increasingly large and complex systems are built to achieve a specific function. However, EMI analysis is more problematic in this kind of complex system due to the difficulty in source identification in conjunction with the high frequency. In general, near-field scanning methodology is often used for root cause diagnostics to find the source of EMI radiation [1]. This method can provide us the reactive near field distribution on the Device under test (DUT). However, in practice the near-field technique has difficulties in placing the probe close enough to the complex and sensitive DUT. Furthermore, EMC engineers are primarily concerned with the sources of EMI contributing to far-field radiation only, which near field scanning is often not capable of identifying [1]. The emission source microscopy (ESM) technique provides a powerful tool to detect and characterize the active sources of radiation in a complex system. In this method, the amplitude and phase of fields are measured on a plane away from the DUT. The ESM algorithm is then applied to propagate the fields back to the source plane and to localize the sources of radiation. After performing source localization the non-conductive wideband absorber material is used to reduce the EMI. By placing the lossy material on the source location it can effectively reduce the radiation over a broadband frequency range, without requiring additional design changes to the DUT. The lossy material is utilized to mitigate the EMI problems at 10 GHz.

The viability and effectiveness of method is confirmed by comparison with the total radiated power calculated from the scanning data as well as the measurement in a reverberation chamber.

II. EMISSION SOURCE MICROSCOPY

In literature, synthetic aperture radar techniques are mainly used for antenna diagnostics and antenna pattern measurement [2]. Such techniques have also been used for microwave imaging to detect concealed objects and structural defects [3][4]. Standard SAR methods use signals reflected from the target and received by a scanning antenna to reconstruct the target's image. In this work, ESM algorithm based on SAR technique is used to identify active sources of radiation on a PCB. The ESM algorithm can be summed up using the following equation [4] (in the assumption that the scan is done on the x-y plane parallel to the source plane),

$$E_t^0(x,y,0) = \mathbf{F}^{-1}\left[\mathbf{F}\left\{E_t(x,y,z_0)\right\} \times \mathrm{e}^{-\mathrm{j}k_z z_0}\right] \qquad (1)$$

where $E_t(x, y, z_0)$ is the tangential field on scanning plane,
$E_t^0(x, y, 0)$ is the reconstructed field on source plane,
z_0 is the distance to be translated,
$k_z = \sqrt{k_0^2 - k_x^2 - k_y^2}$ is the component of the propagation vector,

where k_x, k_y, k_z are the components of the propagation vector,
$k_0 = 2\pi/\lambda$ is the free space wavenumber,
$\mathbf{F}$ and $\mathbf{F}^{-1}$ are the forward and reverse Fourier transform operators respectively.

To implement (1) the measured tangential field components are converted to spatial spectral domain using a 2D fast Fourier transform and multiplied by the phase term to translate the fields back to the source plane. The non-propagating field component can be suppressed in the spectrum domain. On the source plane, the original fields can again be reconstructed from the spectrum by using an inverse 2D-FFT. The rectangular scanning plane is divided into a grid of N × M points. The separation of sampling points on the scanning grid is chosen to be less than $\lambda/2$ in order to satisfy the Nyquist spatial sampling criterion as recommended in [5].

III. Lossy Material Characteristics

The properties of the absorber material are defined by the permittivity and permeability. Any use of absorber involves a trade-off between material absorptivity and impedance matching at the surface [6]. Finding a suitable absorber material for the desired frequency range will improve the effectiveness of the absorber and thus reduce the total volume of the material required. In this work, for frequencies at 10 GHz, a non-conductive, magnetically lossy material (BSR-2) [7] was used for EMI mitigation.

IV. Source Location Identification on the Real Hardware

The DUT used for analysis in this paper is an off-the-shelf networking device with default software configuration installed. Fig. 1 shows the measured radiation spectrum from the DUT. This measurement is performed by operating the DUT in a reverberation chamber and measuring the total radiated power using a spectrum analyzer. It can be seen that there are 15 peaks in the spectrum centered at 10.3125 GHz. This paper presents a case study on the mitigation of radiation corresponding to only a single frequency i.e. frequency #12 at about 10.312584 GHz. Similarly this analysis can also be extended to other frequency components.

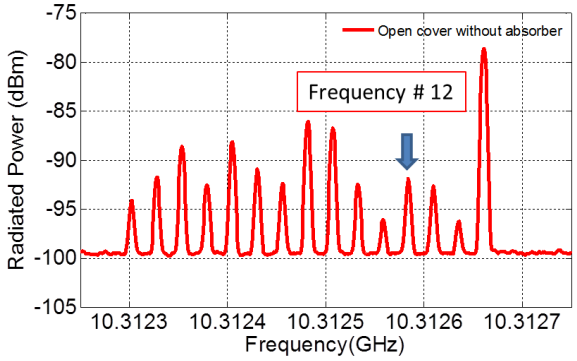

Fig. 1. Radiation spectrum from the DUT

The test setup for the hardware measurement using the ESM technique is as shown in Fig. 2.

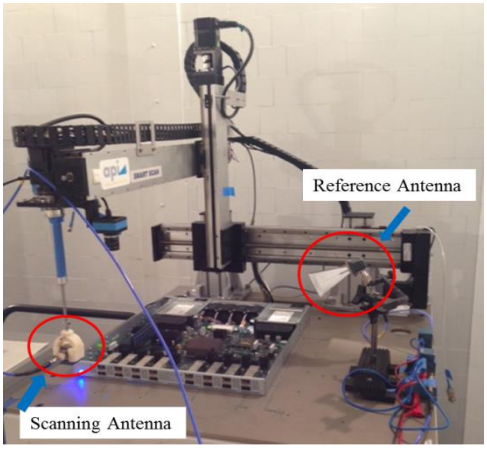

Fig. 2. ESM test setup for the real hardware measurement

The DUT with dimensions of 45 cm × 40 cm × 4 cm is placed at the center of a 3-axis robotic scanning system [8]. At this frequency the required maximal spatial scanning step is 1.5 cm. In the actual measurement, a scanning resolution of 7 mm is used. The height of the scanning plane above the PCB is about 8.3 cm, which is between two to three wavelengths at the test frequency.

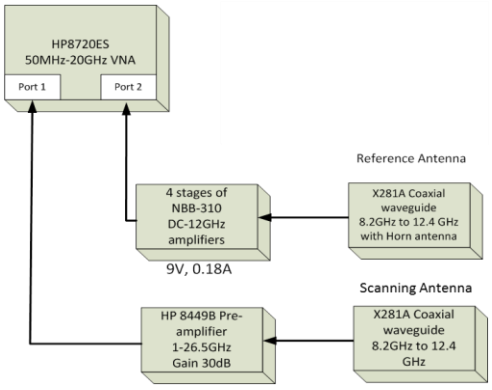

Fig. 3. The schematic diagram of the ESM measurement setup

For the ESM method, the tangential amplitude and phase information on the scanning plane are enough to calculate the field pattern on the source plane. A vector network analyzer (VNA) is used in the tuned receiver mode for phase and amplitude measurement. In this mode, one port of the VNA is connected to the reference signal and second port is connected to the signal to be measured. Fig. 3 shows the schematic diagram of the ESM measurement setup.

For this measurement, an 8.2-12.4 GHz standard gain horn antenna was used as a reference antenna. This reference antenna is fixed at a distance away from the DUT in the direction to maximize the output at frequency #12. It is connected to Port 2 of VNA through three cascaded DC-12 GHz amplifiers each providing 10 dB gain. The scanning antenna is an 8.2-12.4 GHz open-ended waveguide mounted to the arm of the 3-axis robotic scanning system. The output of the waveguide is amplified by a low noise broadband amplifier with a gain of 30 dB before feeding to Port 1 of the VNA. The scanning antenna moves over a scanning plane in a rectangular grid and measures one tangential component of the field in one scan. To measure the orthogonal field component, the antenna is rotated 90 degrees and the scan is repeated.

The image of the DUT is overlapped and aligned with the image of the scanned fields to observe the underlying physical sources of radiation as shown in Fig. 4. In this figure, the DUT image has been replaced by the blocks due to the proprietary information. Four big black blocks represents the heatsinks in the DUT, 16 smaller blue blocks with the same size represents the physical layer transceiver (PHY), and 8 red rectangular blocks corresponds to the optical transceivers on the DUT. As observed, no detailed information about the source of radiation can be obtained from the scanned fields. The quantity plotted is the magnitude and phase of the signal at the VNA Port 1, and the units are dBV and radians respectively.

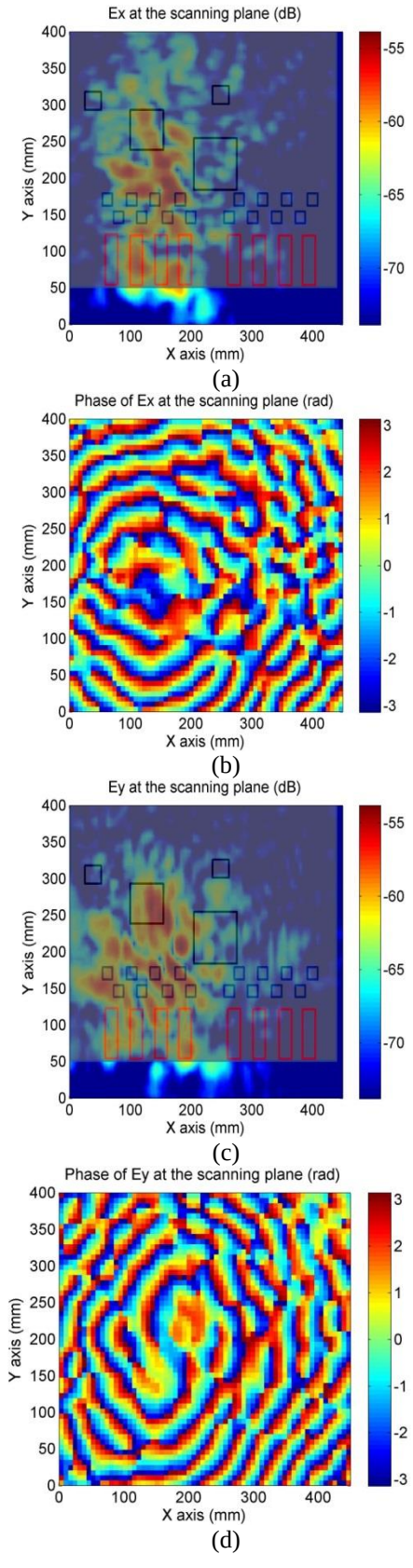

Fig. 4. (a) Measured E_x field magnitude in dBV (b) Measured E_x field phase in rad (c) Measured E_y field magnitude in dBV (d) Measured E_y field phase in rad at the scanning plane.

Also a near-field scanning using a near-field magnetic field probe is performed for frequency #12, as shown in Fig. 5. The scanning height is kept as 2 mm above the PCB plane. Here the scanning resolution is kept as 1 mm and only a small area is scanned due to the large time required for scanning. It provides the surface current distribution corresponding to frequency # 12. Also it contains both the evanescent and propagating wave components. No particularly useful information about the radiating structure can be obtained from the field data. This is not enough to decide where exactly to put the absorbers to reduce the far-field radiation.

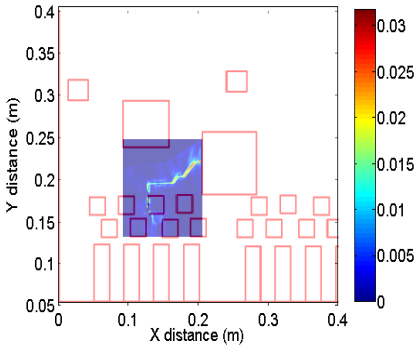

Fig. 5. Measured total tangential field component magnitude in dBm.

To identify the source location, ESM algorithm as given by (1) is applied on the scanned fields shown at Fig. 4. The reconstructed fields on the source plane for both orientations of the antenna are shown in Fig. 6.

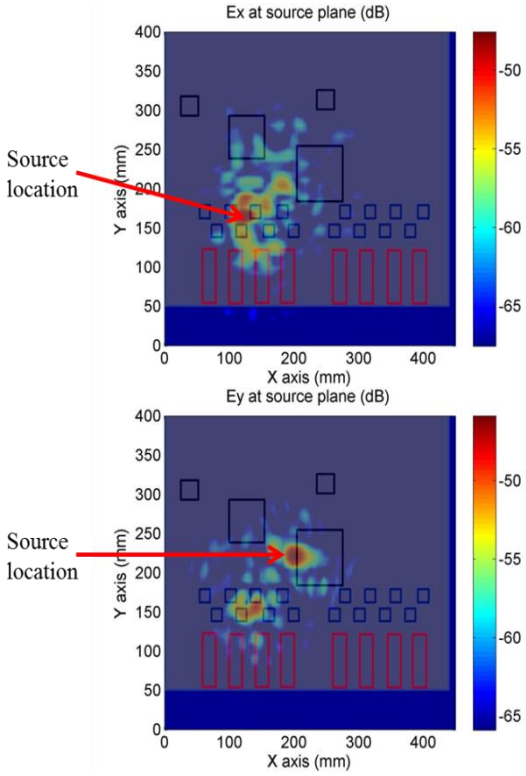

Fig. 6. Reconstructed E_x and E_y field component magnitude in dBm at the PCB plane.

The resolution of the reconstructed image can be estimated as 1.5 cm according to [10]. Here it can be seen that for the radiation in *x* direction, the source is mainly located near one of the PHYs of the board; and for the radiation in *y* direction, the source is mainly located at the edge of the main heatsink.

V. EMI MITIGATION WITH LOSSY MATERIAL

Based on the information obtained from the ESM transformation, we can identify a suitable position for placing the absorber material to mitigate the radiation at frequency #12. Four pieces of absorber material are placed on the edge of the main heatsink where the hot spot corresponding to the source of radiation can be observed as marked in Fig. 6 (b). Each piece of absorber material size is 2 cm by 2.8 cm, with the thickness 1 mm. The placement of the absorber material is as shown in Fig. 7.

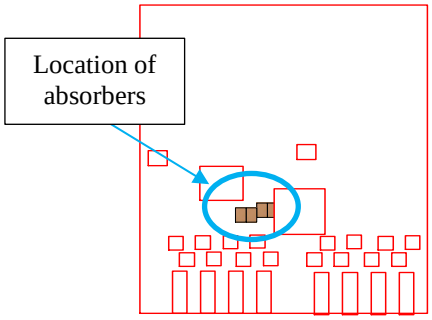

Fig. 7. Applied absorbers (2 cm by 2.8 cm)

Fig. 8 shows the reconstructed image from the source plane, after the absorber materials are added at the source location. The color scale corresponding to the field strength in Fig. 8 is set to be the same as Fig. 6 to facilitate comparison. It can be clearly observed that the field strength at the source location has been greatly reduced due to the effect of the absorber material. This validates the location of the source identified by the ESM algorithm to be accurate.

By comparing the reconstructed field strengths in the source plane with and without the absorber material, the maximum value of the source in the *x* orientation is reduced from -47.6 dB to -53.9 dB, when the absorber material is added; for the *y* orientation, the maximum value of the source is also reduced from -45.9 dB to -49.9 dB.

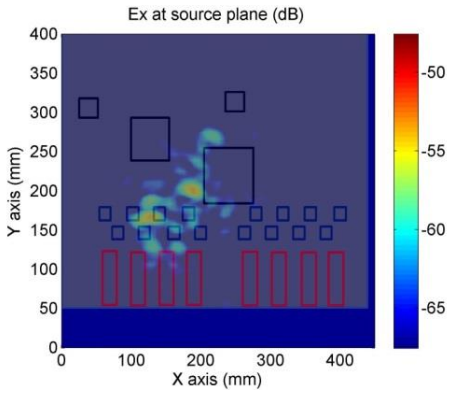

Fig. 8 a) Reconstructed E_x fields at the PCB plane, with absorber.

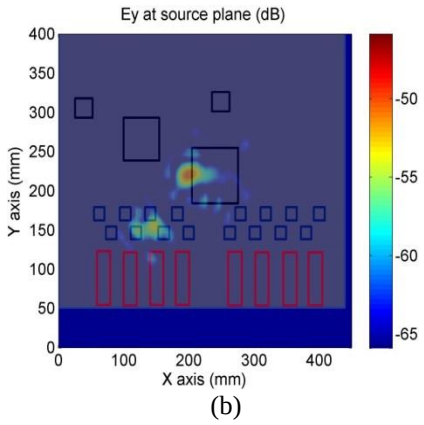

Fig. 8 a) Reconstructed E_y fields at the PCB plane, with absorber.

VI. TOTAL RADIATED POWER COMPARISON

As seen from the previous results, it can be observed that the source radiation is reduced by approximately 4 dB when the absorber material is placed at the location identified by the ESM algorithm. To validate these results in the far-field, a total radiated power measurement (TRP) is performed on the DUT using a reverberation chamber. The reverberation chamber measurement is widely used for EMI testing and particularly effective in quantifying the total radiated power of the DUT [11]. Fig. 9 shows the setup for the TRP measurement of the DUT. A spectrum analyzer is used with center frequency at 10.3125 GHz and the span as 500 kHz. A low noise 30 dB broadband amplifier is used to increase the received signal strength. Fig. 10 shows the averaged total radiated power spectrum comparison with and without absorber material.

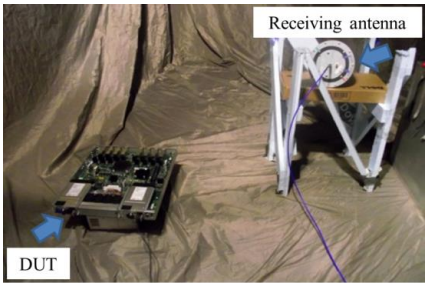

Fig. 9. Setup for the TRP measurement in a reverberation chamber

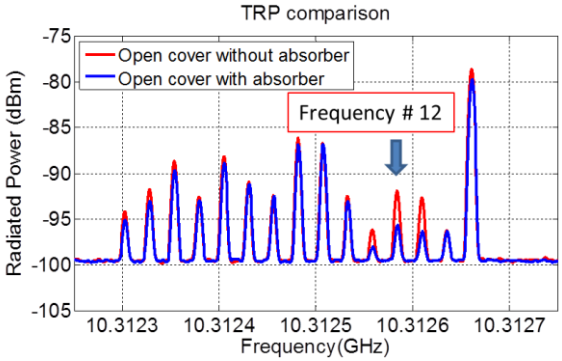

Fig. 9. TRP spectrums comparison with and without the absorber material.

From the Fig. 10, it can be seen that the peak value corresponding to frequency #12 has reduced about 4 dB, due to the absorber material, which validates the previous measurement using the ESM method. But as observed, most of the other frequencies are not affected by the placement of the absorber material. This reconfirms that the location of absorber material determined by the ESM algorithm mainly corresponds to the source of frequency # 12.

VII. CONCLUSION

Using emission source microscopy technique, sources of EMI radiation can be approximately localized on a complex and large system. By placing a suitable volume absorber material on the identified source location, the EMI radiation at 10 GHz from a particular source can be reduced. A TRP measurement using the reverberation chamber method validates the reduction of radiation from the identified source. This method can be extrapolated to identify the source of other frequency components as well.

ACKNOWLEDGMENT

This material is based upon work supported by the National Science Foundation under Grant No. 0855878.

REFERENCES

[1] A. D. Yaghjian, "An overview of near-field antenna measurements," *IEEE Transactions on Antennas and Propagation*, vol. 34, no. 1, pp. 30-45, 1986.

[2] P. L. Ransom, and R. Mitra, "A method of locating defective elements in large phased arrays," *Proc. of the IEEE*, vol. 59, no. 6, pp. 1029-1030, 1971.

[3] M. Fallahpour, M. Ghasr, J.T. Case, and R. Zoughi, "A Wiener Filter-Based Synthetic Aperture Radar (SAR) Algorithm for Microwave Imaging of Targets in Layered Media", *Materials Evaluation*, vol. 69, no. 10, pp. 1227-1237, Oct. 2011.

[4] D. M. Sheen, D. L. McMakin, and T. E. Hall, "Three-dimensional Millimeter-Wave Imaging for concealed Weapon Detection," in *IEEE Transactions on Microwave Theory and Techniques*, vol. 49, no. 9, pp. 1581-1592, 2001.

[5] J. T. Case, M. T. Ghasr, and R. Zoughi, "Optimum Two-Dimensional uniform spatial sampling for microwave SAR-Based NDE imaging," *IEEE Transactions on Instrumentation and Measurement*, vol. 60, no. 12, pp. 3806-3815, 2011.

[6] M. Saitoh, T. Yamamoto, T. Sakamoto, H. Niori, M. Chino, and M. Kobayasi, "Electromagnetic wave absorber using dielectric (Ti)·magnetic(Fe) composite material for GHz frequency band," *Proceedings of the 12th IEEE International Symposium on Applications of Ferroelectrics*, vol. 2, pp. 871-874, 2000.

[7] Laird Technologies, "Microwave Absorber: ECCOSORB," [Online]. Available: http://www.eccosorb.com/products-eccosorb-bsr.htm

[8] G. Muchaidze, J. Koo, Q. Cai, T. Li, L. Han, A. Martwick, K. Wang, J. Min, J. L. Drewniak, and D. Pommerenke, "Susceptibility Scanning as a Failure Analysis Tool for System-Level Electrostatic Discharge (ESD) Problems," *IEEE Transactions on Electromagnetic Compatibility*, vol. 50, no. 2, pp.268-276, 2008.

[9] K. Wang; D. Pommerenke, J. M. Zhang, and R. Chundru, "The PCB level ESD immunity study by using 3 dimension ESD scan system," *International Symposium on Electromagnetic Compatibility*, vol. 2, pp.343-348, 2004.

[10] M. Abramowitz and M. W. Davidson, "Microscope Objectives: Numerical aperture and resolution," *Molecular Expressions: Optical Microscopy Primer* (website), Florida State University, April, 2004.

[11] G. Koepke and J. Ladbury, "Radiated Power Measurements in Reverberation Chambers," 56th ARFTG Conference Digest-Fall, vol. 38, pp.1-7, 2000.